Advanced Composite Materials, 2015
http://dx.doi.org/10.1080/09243046.2014.985420

Taylor & Francis
Taylor & Francis Group

New analytical method for electric current and multiple delamination cracks for thin CFRP cross-ply laminates using equivalent electric conductance

Akira Todoroki*

Department of Mechanical Sciences and Engineering, Tokyo Institute of Technology, 2-12-1 Ookayama, Meguro-ku, Tokyo 152-8552, Japan

(*Received 11 July 2014; accepted 22 September 2014*)

Carbon fiber reinforced polymer (CFRP) composites have low inter-lamina strength. One of the monitoring technologies is a self-sensing method that uses the electrical resistance change of a CFRP structure for detecting damage. The electric current distribution is vital information for the self-sensing method when optimizing the arrangement of probes to measure electric potential changes. We have developed a new orthotropic electric potential function analysis approach using affine transformation for unidirectional CFRP. In this study, the orthotropic electric potential function analysis method is improved to calculate the electric current of a thin cross-ply CFRP. Two types of stacking sequences for the beam-type cross-ply laminates were calculated to confirm the effectiveness of the improved method. The electrical voltage changes caused by multiple delamination cracks of a cross-ply laminate are new outcomes of this study. The analytical results were compared with computed results using the finite difference method. Consequently, the new equivalent electric conductance method proved to be effective for calculations of the electric current density of a cross-ply CFRP laminate. Furthermore, the new method for calculating the electric potential difference changes caused by multiple delamination cracks using orthotropic distributed doublet analysis, with the equivalent electric conductance, has also proved to be effective.

Keywords: carbon fiber; polymer composites; electric conductance; laminates; delamination

1. Introduction

Carbon fiber reinforced polymer (CFRP) composites have high strength and stiffness to weight ratios compared with conventional metallic materials. The advantages broaden the applications of CFRP composites from aerospace structures to other transportation vehicles such as automobiles and trains. The laminated CFRP structures, however, have low inter-lamina strength, which can result in delamination cracks from any low-velocity impact loads. As the delamination is difficult to detect from visual inspection, adequate delamination monitoring systems are essential for CFRP structures. One of the monitoring methods is the self-sensing method that uses electrical resistance change for damage

*Email: atodorok@ginza.mes.titech.ac.jp

This article was originally published with errors. This version has been corrected. Please see Corrigendum (http://dx.doi.org/10.1080/09243046.2015.1032502).

detection. The method uses the carbon fibers as sensors. Many research articles have been published on detecting the damage in CFRP composite laminates.[1–15]

For the self-sensing method, the electric current distribution is important information for optimizing the arrangement of detecting probes. The electric current analysis is not easy because of the strongly orthotropic electric conductance of the CFRP laminated composites. As a consequence a large number of divided elements in the thickness orientation for the finite element method (FEM) are required. This implies that in practice FEM analysis of CFRP laminates is extremely costly.

We have developed a new orthotropic, electric potential, function analysis approach using affine transformation for unidirectional CFRP.[16] Using the orthotropic electric function, the electric current density and potential distribution can be obtained for thick unidirectional CFRP. Even for a thick cross-ply laminate, the analysis method provided good estimates with the assumption that the electrical potential distribution in the thickness direction is the same as that for unidirectional CFRP. A new lamination theory for a thick CFRP laminate that has electric potential distribution in the thickness direction was proposed and proved to be effective.[17] For thin unidirectional CFRP, a mirror-image analysis method was applied that showed excellent results, and the method was extended to the electric potential analysis of unidirectional CFRP with a delamination crack using a distributed orthotropic doublet method.[18] A new analysis-based method to identify the location and dimension of delamination cracks was proposed.[19]

These previous studies did not include a thin cross-ply laminate. In the present study, therefore, the analysis method was improved for calculating the electric current of a thin cross-ply CFRP. Two types of stacking sequences of beam-type cross-ply laminates were calculated to confirm the effectiveness of the improved method. Electrical voltage changes after delamination cracking of a cross-ply laminate were calculated in the present study. The analyzed results were compared with the computed results using the finite difference method (FDM).

2. Analysis method

2.1. Electric current analysis using the orthotropic electric potential function.[16]

The orthotropic electric potential function method [16] is briefly explained in this section. Let us consider the two-dimensional case with Cartesian coordinates of $x-z$. The electric conductance for the x-orientation is σ_x and z-orientation is σ_z. The electric potential is f. The electric current density for the x-direction i_x and z-direction is i_z, and are obtained as follows:

$$i_x = -\sigma_x \frac{\partial \phi}{\partial x}, \quad i_z = -\sigma_z \frac{\partial \phi}{\partial z}. \tag{1}$$

For the steady-state electric current, the continuity of current gives the following equation:

$$\sigma_x \frac{\partial^2 \phi}{\partial x^2} + \sigma_z \frac{\partial^2 \phi}{\partial z^2} = 0. \tag{2}$$

We now use the following affine transformation:

$$\xi = \frac{x}{\sqrt{\sigma_x}}, \quad \eta = \frac{z}{\sqrt{\sigma_z}}. \tag{3}$$

Using the affine transformation of Equation (3), Equation (2) can be transformed in the following Laplace equation:

$$\frac{\partial^2\phi}{\partial\xi^2}+\frac{\partial^2\phi}{\partial\eta^2}=0. \tag{4}$$

The transformed Equation (4) indicates that the electric current flow is similar to the potential flow of a perfect fluid without a vortex. In the infinite $x-z$ coordinate plane, the electric current density an electric current source and sink pair is given as follows:

$$i_x=\frac{I}{2\pi\sqrt{\sigma_x\sigma_z}}\left\{\frac{x+a}{\frac{(x+a)^2}{\sigma_x}+\frac{z^2}{\sigma_z}}-\frac{x-a}{\frac{(x-a)^2}{\sigma_x}+\frac{z^2}{\sigma_z}}\right\},\quad i_z=\frac{I}{2\pi\sqrt{\sigma_x\sigma_z}}\left\{\frac{z}{\frac{(x+a)^2}{\sigma_x}+\frac{z^2}{\sigma_z}}-\frac{z}{\frac{(x-a)^2}{\sigma_x}+\frac{z^2}{\sigma_z}}\right\} \tag{5}$$

where a source is located at $(x, z) = (-a, 0)$, and a sink located at $(a, 0)$.

When an electric current source and sink pair exists in a thin CFRP laminate as shown in Figure 1, the electric current can be calculated using multiple mirror images of the pairs of sources and sinks.

Figure 2 shows the schematic representation of the mirror images of the sources and sinks.[18] In this study, the image is limited to the z-direction because the thickness is the most important issue. If the beam is not long enough, multiple mirror images should be placed in both ends to the right and left. The cross-sectional view given in Figure 1 is identical to the bottom half of part of the thickness $2t$ in the area of $N = 0$ in Figure 2. In this figure, N denotes the number of sets of plus and minus images. For example, $N = 10$ includes the image from #−10 to #10. If N sets of images are required, the electric current density is obtained by summing up the electric current densities from the image of #$-N$ to that of #N:

$$\begin{aligned} i_x&=\sum_{k=-N}^{N}\frac{I}{\pi\sqrt{\sigma_x\sigma_z}}\left\{\frac{x+a}{\frac{(x+a)^2}{\sigma_x}+\frac{(z-2tk)^2}{\sigma_z}}-\frac{x-a}{\frac{(x-a)^2}{\sigma_x}+\frac{(z-2tk)^2}{\sigma_z}}\right\},\\ i_z&=\sum_{k=-N}^{N}\frac{I}{\pi\sqrt{\sigma_x\sigma_z}}\left\{\frac{z-2tk}{\frac{(x+a)^2}{\sigma_x}+\frac{(z-2tk)^2}{\sigma_z}}-\frac{z-2tk}{\frac{(x-a)^2}{\sigma_x}+\frac{(z-2tk)^2}{\sigma_z}}\right\}\end{aligned} \tag{6}$$

2.2. *Analysis of a delamination using an orthotropic doublet line [18]*

As the electric potential function is isotropic for the $\xi-\eta$ coordinate, a plate in a flow field can be produced using the placement of a distributed double flow that eradicates

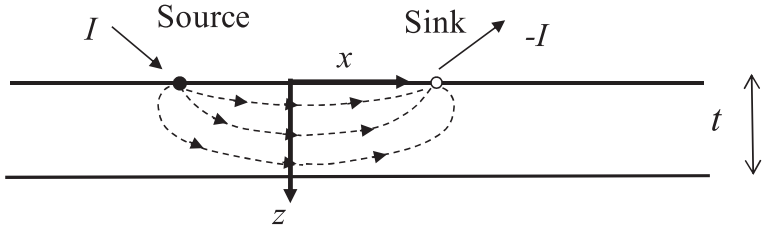

Figure 1. Source and sink model for electric current analysis of laminate composites.

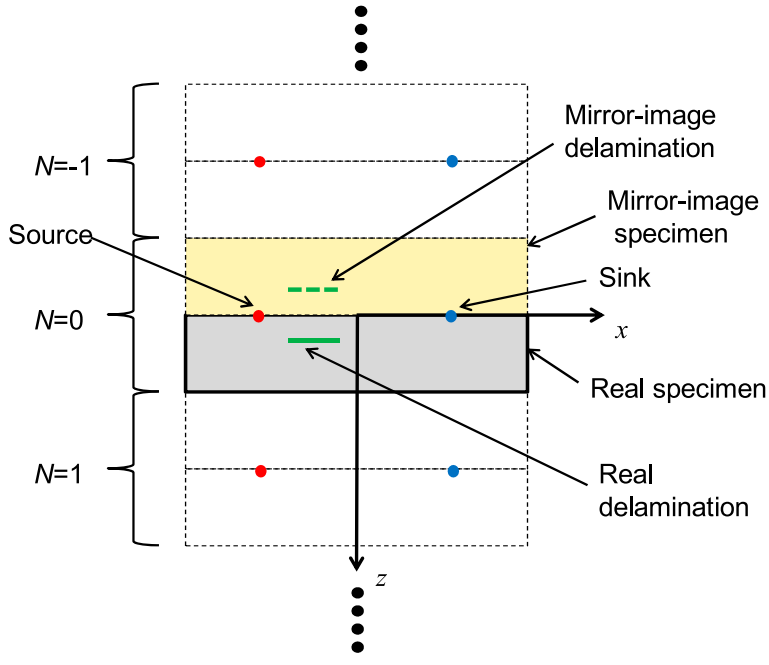

Figure 2. Schematic representation of mirror-image analysis.

flow perpendicular to the plate. The plate in the flow corresponds to a crack in the electric current flow. To eradicate the electric current perpendicular to the crack plane, a distributed doublet must be placed on the crack surface.

Using the illustration in Figure 3, we now consider a delamination crack that is located between $(x_1, 0)$ and $(x_2, 0)$. The location $z = 0$ is not the top surface of the specimen but in this case is moved to the crack location. To eradicate the electric current flow perpendicular to the crack, a distributed double flow that has flow perpendicular to the x-coordinate must be placed on the crack, as shown in Figure 3. To eradicate the electric current perpendicular to the crack surface, a distribution of a doublet of the strength of $\mu(x)$ is placed on the crack surface. To determine the strength distribution $\mu(x)$ of the doublet, the integral equation must be solved so that eradication of the electric current is achieved.

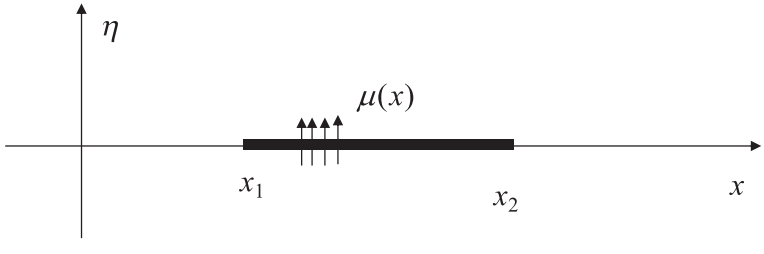

Figure 3. Distributed doublet model to calculate the delamination effect.

Let $i_z(x, z)$ be the electric current density at the source and sink, $i_{z,crack}(x, z)$ is the electric current density at a crack (a real delamination crack is considered here for simplicity), and d is the depth of the delamination crack from the surface:

$$i_{z,crack}(x,z) = -\frac{\sqrt{\sigma_z}}{2\pi}\int_{x1}^{x2}\mu(s)\frac{\left(\frac{x-s}{\sqrt{\sigma_x}}\right)^2-\left(\frac{z-d}{\sqrt{\sigma_z}}\right)^2}{\left\{\left(\frac{x-s}{\sqrt{\sigma_x}}\right)^2+\left(\frac{z-d}{\sqrt{\sigma_z}}\right)^2\right\}^2}ds. \tag{7}$$

The integral equation is given as follows:

$$i_z(x,d) + i_{z,crack}(x,d) = 0 \tag{8}$$

As shown in Figure 3, the z-coordinate is moved parallel to the doublet center. The translation implies setting $z = d$ in Equation (7) giving:

$$i_z(x,0) - \frac{\sigma_x\sqrt{\sigma_z}}{2\pi}\int_{x1}^{x2}\frac{\mu(s)}{(x-s)^2}ds = 0. \tag{9}$$

Equation (9) is a hypersingular integral equation. Thus, after obtaining the doublet distribution $\mu(x)$, the electric voltage change caused by the delamination crack can be calculated using Equation (10):

$$V(x,z) = 2\{\varphi(x,z) - \varphi_0(x,z)\} = -\frac{1}{\pi\sqrt{C_x}}\int_{x1}^{x2}\mu(s)\frac{\left(\frac{z}{\sqrt{\sigma_z}}\right)}{\left(\frac{x-s}{\sqrt{C_x}}\right)^2+\left(\frac{z}{\sqrt{\sigma_z}}\right)^2}ds \tag{10}$$

where ϕ_0 is the electric potential before delamination cracking. In this calculation, only one mirror image of the doublet is considered because the flow it causes is very small. The electric potential ϕ, therefore, is doubled because we have the real delamination crack and image delamination crack of $N = 0$ in Figure 2.

2.3. New analysis using an equivalent conductance for a cross-ply laminate

Figure 4 shows the configuration of a specimen 40-mm long and 2-mm thick. The longitudinal direction of the beam-type specimen is defined as the x-coordinate, which is defined as the 0° of carbon fiber orientation.

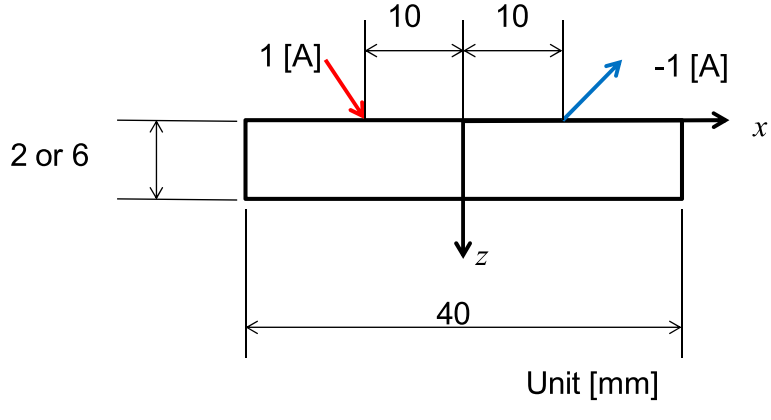

Figure 4. Specimen configuration.

Electrical density at $x = 0$ (the center of the specimen) of a cross-ply laminate $[(0/90)_4]s$ is calculated using an electric potential difference calculated from the unidirectional CFRP of 0°-plies. Figure 5 shows the calculated results for the electric current density. The ordinate is the electric current density in the x-direction (i_x) at the center ($x = 0$), and the abscissa is the depth (z) from the surface where the electric current is applied. The solid curve is the numerical computational result using a FDM. The broken curve is the calculated electric current density obtained from the electric potential difference distribution of the unidirectional CFRP. A comparison shows that the electric current density calculated using the electric potential difference distribution from the unidirectional CFRP does not agree with the FDM results. This means the electric potential difference of the cross-ply laminate is different from that of the unidirectional CFRP of 0°-plies. To obtain the exact electric current density of a cross-ply laminate, the electric potential difference of a cross-ply laminate must be obtained.

Equation (6) gives the electric current density distribution and Equation (1) gives the electric potential difference when an electric current density exists. For the cross-ply laminate, although the electric conductance in the thickness direction is the same as for unidirectional CFRP, the conductance in the x-direction is different from that of the fiber direction of the unidirectional CFRP.

We assume that the electric potential difference distribution of a cross-ply laminate can be calculated using Equations (1) and (6) when an appropriate electric conductance is obtained. To obtain the electric potential difference distribution of the cross-ply laminate, an equivalent conductance is assumed, which provides it with an almost equal electric potential distribution. When an electric current is applied to the surface of the CFRP plate, the electric potential difference is not uniform in the thickness direction. This non-uniform electric potential difference requires special measures in the lamination theory of electric conductance of CFRP laminates.[17]

Figure 6 shows the uniform electric potential difference and the actual non-uniform distribution. The non-uniform distribution means the bottom of the CFRP laminate is not used effectively for the electric current path when the electric current is applied to the surface. To consider this effect, Ref. [17] proposed a contribution function to calculate the electric conductance of a CFRP laminate. The contribution function is the

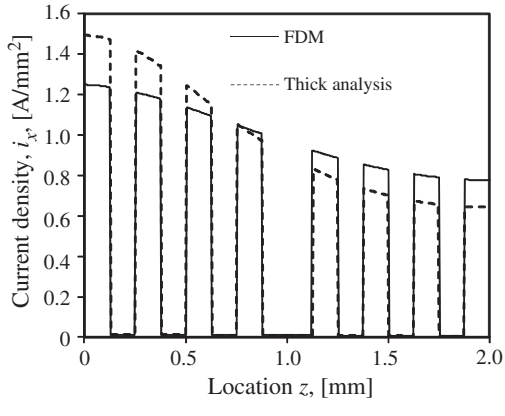

Figure 5. Comparison of the electric current density calculated using the electric potential difference of unidirectional CFRP.

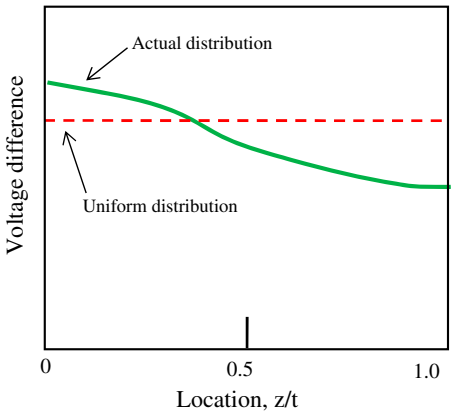

Figure 6. Model of the actual distribution of electric potential difference (voltage difference).

normalized electric potential difference. The small value of the contribution function at the normalized depth α (=z/t, t: the thickness of the laminate) means the area at the thickness α is small for the electric current as shown in Figure 7. Therefore, the width of the area at α virtually shrunk, and the electric conductance of the laminate can be calculated.

To obtain the equivalent conductance for calculating the electric current density of a cross-ply laminate, the contribution function from Ref. [17] is available. The calculation of the contribution function, however, requires the distribution of electric potential difference and its calculation requires the equivalent electric conductance. In this study, therefore, an iteration method is adopted to obtain the equivalent electric conductance as follows:

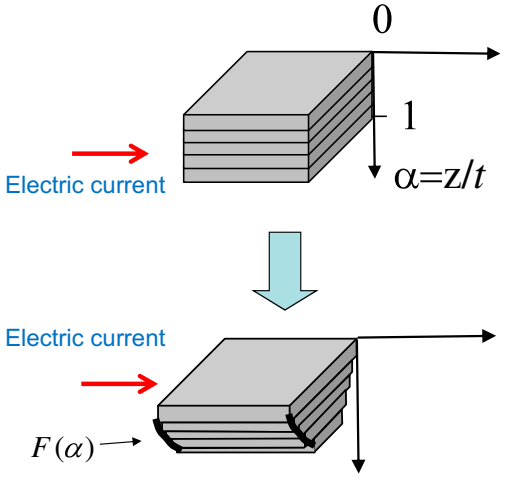

Figure 7. The definition of the contribution function to calculate the equivalent electric conductance.

(1) Using a unidirectional 0°-ply laminate, the electrical potential difference is calculated using Equations (1) and (6) at the center $x = 0$.
(2) A normalized contribution function $F(\alpha)$ is obtained from the calculated electrical potential difference at the M-divided points of the z-coordinate.
(3) Using the obtained contribution function $F(\alpha)$, the equivalent electric conductance C_x is calculated using the method described in Ref. [17]:

$$C_x = \int_0^1 F(\alpha)\sigma_x d\alpha. \tag{11}$$

(4) When the obtained equivalent electric conductance C_x is different from the previously calculated C_x over the allowable limit value, recalculate the electric potential difference again using Equations (1) and (6) with the obtained C_x. When the C_x has a small difference compared with the allowable limit value, the iteration is terminated and the C_x is assumed to be the equivalent electric conductance.

In the present study, the number of divisions M is set to 100 at each ply to calculate the contribution function.

For the cross-ply laminates, the electric potential difference can be calculated by the substitution of the obtained equivalent electric conductance C_x into σ_x of Equations (1) and (6). From the calculated electric potential difference, the electric current density can be calculated using the actual electric conductance σ_0 or σ_{90} with Equation (1).

2.4. New analysis of a delamination crack in a cross-ply laminate

In this study, $z = d - \varepsilon$ is set in Equation (7) to prevent the hypersingularity: ε is a small number compared with the ply thickness. Because the ply thickness is 0.125 mm, the sufficiently small difference ε is set to 0.03 mm. The delamination area is divided into small segments 0.2-mm long. To calculate the doublet strength for each segment, it is assumed to be uniform in each small segment. Let the total number of divisions of the integral be n_s. To calculate the doublet strength, i_z is eradicated at the center of each segment (x_{cj}).

$$i_z(x_{cr}, d) - \sum_{j=0}^{ns} \mu_j \int_{xj}^{xj+1} \frac{\sqrt{\sigma_z}}{2\pi} \frac{\left(\frac{x_{cr}-s}{\sqrt{C_x}}\right)^2 - \left(\frac{\varepsilon}{\sqrt{\sigma_z}}\right)^2}{\left\{\left(\frac{x_{cr}-s}{\sqrt{C_x}}\right)^2 + \left(\frac{\varepsilon}{\sqrt{\sigma_z}}\right)^2\right\}^2} ds = 0, \tag{12}$$

where $i_z(x_{cj}, d)$ is i_z at the center of each segment. Equation (12) gives a set of simultaneous linear equations. Solving the simultaneous linear equations, the set of doublet strength (μ_j) can be obtained and the electric potential difference caused by a delamination crack is calculated using the discretized Equation (10). Note that σ_x is replaced by the equivalent electric conductance C_x in Equation (12).

To calculate the change in electric potential difference on the surface of the specimen after delamination cracking, the equivalent electric conductance C_x is substituted for σ_x in Equation (12) to calculate the doublet strength μ_j. To calculate the

change in electric potential difference, the equivalent electric conductance C_x is substituted for σ_x in Equation (9).

When multiple delamination cracks exist, the segment division is extended to the edge of the right tip of the last delamination crack. We now consider that the two delamination cracks exist. The left edge of the first delamination crack is x_0 and the right edge is x_k. The left edge of the second delamination crack is $x_p (x_p > x_k)$ and the right edge is x_q. We calculate the integral of Equation (12) as follows:

$$B_{jr} = \int_{xj}^{xj+1} \frac{\sqrt{\sigma_z}}{2\pi} \frac{\left(\frac{x_{cr}-s}{\sqrt{C_x}}\right)^2 - \left(\frac{\varepsilon}{\sqrt{\sigma_z}}\right)^2}{\left\{\left(\frac{x_{cr}-s}{\sqrt{C_x}}\right)^2 + \left(\frac{\varepsilon}{\sqrt{\sigma_z}}\right)^2\right\}^2} ds. \tag{13}$$

The simultaneous linear equations can be written in matrix form as follows:

$$\begin{pmatrix} B_{1,1} & \cdots & B_{1,k} & B_{1,p} & \cdots & B_{1,q} \\ \vdots & \ddots & \vdots & \vdots & \ddots & \vdots \\ B_{k,1} & \cdots & B_{k,k} & B_{k,p} & \cdots & B_{k,q} \\ B_{p,1} & \cdots & B_{p,k} & B_{p,p} & \cdots & B_{p,q} \\ \vdots & \ddots & \vdots & \vdots & \ddots & \vdots \\ B_{q,1} & \cdots & B_{q,k} & B_{q,p} & \cdots & B_{q,q} \end{pmatrix} \begin{pmatrix} \mu_1 \\ \vdots \\ \mu_k \\ \mu_p \\ \vdots \\ \mu_q \end{pmatrix} = \begin{pmatrix} i_1 \\ \vdots \\ i_k \\ i_p \\ \vdots \\ i_q \end{pmatrix}. \tag{14}$$

As the inverse matrix $\mathbf{B}^{-1}$ in Equation (14) can be easily calculated, the vector $\boldsymbol{\mu}$ can be easily obtained. After the calculation of $\boldsymbol{\mu}$, the surface electric potential difference change can be calculated as follows:

$$V(x,0) = -\frac{1}{\pi\sqrt{C_x}} \sum_{j=1}^{ns} \mu_j \int_{xj}^{xj+1} \frac{\left(\frac{d}{\sqrt{\sigma_z}}\right)}{\left(\frac{x-s}{\sqrt{C_x}}\right)^2 + \left(\frac{d}{\sqrt{\sigma_z}}\right)^2} ds \tag{15}$$

3. Comparison of results

3.1. Specimen

In this study, the specimen used is a beam type as shown in Figure 4. The specimen is 40-mm long and 2-mm thick. An electric current is applied to the top surface of the specimen (source), and the electric current sink (the ground) is also set to the top surface. The spacing between the electrodes is 20 mm. Two types of stacking sequences are prepared: Type A $[(0/90)_4]s$ and Type B $[(0_3/90)_2]s$. The fiber direction of the 0°-ply is identical to the x-axis direction. As the electric conductance ratio between the σ_x and σ_z is significant for electric current density calculations, the electric conductance in the fiber direction σ_0 is not its actual value. The σ_x is set to 1 S/mm, and that of the transverse direction σ_{90} is set to 0.01. The electric conductance of the thickness direction σ_t is set to 0.01 S/m for the Type A specimen. For the Type B specimen, σ_0 is set to 1 S/mm, that of the transverse direction σ_{90} is set to 0.1 S/m and that of the thickness direction σ_t is set to 0.05 S/m. The difference in the thickness of the specimen is equal to the analysis when using a different conductance ratio because of

the affine transformation of Equation (2). In this study, the thickness of the specimen is fixed at 2 mm.

The density of the electric current in the x-direction i_x is calculated for the Type A and Type B specimens. The calculated results are compared with the computed results obtained using FDM analysis. The density of the electric current in the z-direction at a depth of $z = 0.25$ mm, where the inter-lamina between 0°-ply and 90°-ply exists, is calculated for the Type A specimen. The change in electric potential difference resulting from delamination cracking at the specimen's surface is also calculated using the equivalent electric conductance and the distributed doublet flow. The calculated results are compared with the results of the FDM computations. Two cases of delamination cracking were examined in this study. The first was for a single crack 4-mm-long delamination (the crack edge was located at $x = -6$ mm and $x = -2$ mm). The second was for dual cracks 4- and 2-mm long: the edge of the first crack was located at $x = -6$ mm and $x = -2$ mm (the crack length was 4 mm); the edge of the second crack was located at $x = 2$ mm and $x = 4$ mm (the crack length was 2 mm).

For the FDM computations, 801 grids were placed in the x-direction (grid spacing was 0.05 mm) and 200 grids in the z-direction (grid spacing was 0.005 mm). The FDM computations agreed well with the FEM results and the analysis of unidirectional CFRP.[18]

3.2. *Electric current density*

The obtained equivalent electric conductance was $C_x = 0.51$ for the Type A specimen. Figure 8 shows the results for i_x at the specimen center ($x = 0$) for Type A. The ordinate is i_x at $x = 0$ and the abscissa is the depth from the top surface. The solid curve shows the results of FDM and the open-circle symbols are the calculated results for the equivalent electric conductance. As shown in Figure 8, the calculation using the equivalent electric conductance gives excellent estimates and agrees well with the results of FDM.

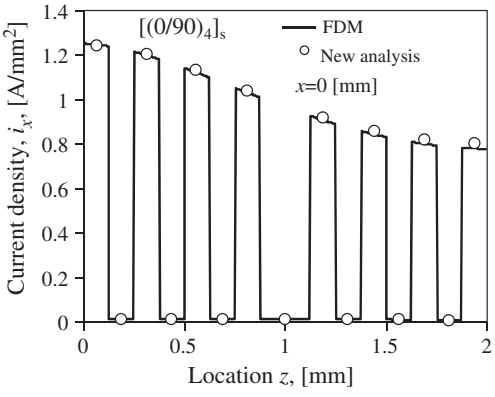

Figure 8. Comparison of the electric current density i_x of Type A at $x = 0$ mm.

Figure 9 shows the results of i_x at $x = 4$ mm for the Type A specimen. As shown in the Section 2.3, C_x is obtained at $x = 0$. Figure 9 shows excellent agreement with the FDM results. Figure 10 shows the results for i_z where they agree very well at all locations. These results mean that the proposed method using the equivalent electric conductance gives excellent estimated results at every location.

The obtained equivalent electric conductance is $C_x = 0.68$ for the Type B specimen. Figure 11 shows the results for i_x at the specimen center ($x = 0$) for Type B. The ordinate is i_x at $x = 0$ and the abscissa is the depth from the top surface. The solid curve shows the results of FDM and the open-circle symbols are the calculated results for the equivalent electric conductance. As shown in Figure 11, the calculation using the equivalent electric conductance gives excellent estimates and agrees well with the results of FDM, even for the different stacking sequences and electric conductance values. The electric conductance in the thickness direction of Type B is 0.05, which is five times greater than for Type A. As shown in Equation (3), the difference in σ_z is similar to the difference in the specimen thickness because of the transformation of the z-axis using σ_z. From this result, the equivalent electric conductance calculation was shown to be effective even for different electric conductance values and specimen dimensions.

3.3. Change in surface electric potential difference resulting from delamination

To confirm the effectiveness of the equivalent electric conductance for the distributed orthotropic doublet analysis, two cases of delamination cracking were investigated for the Type A specimen.

Figure 12 shows the change in electric potential difference after delamination cracking for a single crack case. The ordinate is the change in electric potential difference of the top surface between the intact and delamination cracking cases, and the abscissa is the location of the specimen top surface. The solid curve shows the FDM results and the open-circle symbols indicate the calculated results from the equivalent electric conductance method. Figure 13 shows the results of a dual-crack case. Both results show good agreement between the FDM and calculated results using the equivalent electric conductance method. Because the source and sink points of electric current

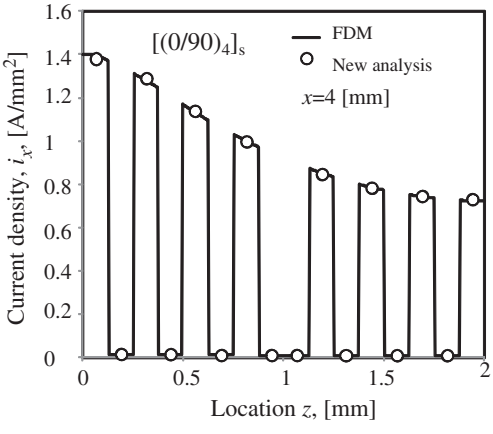

Figure 9. Comparison of the electric current density i_x of Type A at $x = 4$ mm.

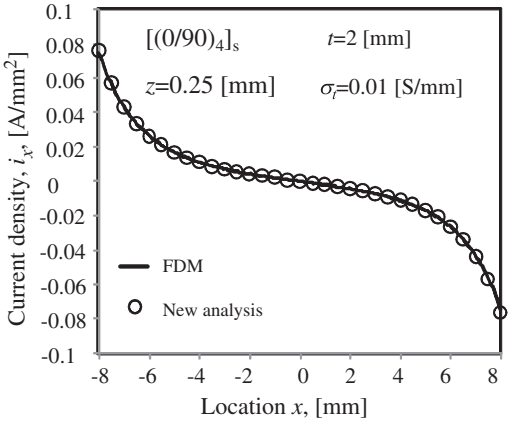

Figure 10. Comparison of the electric current density i_z of Type A at z = 0.25 mm.

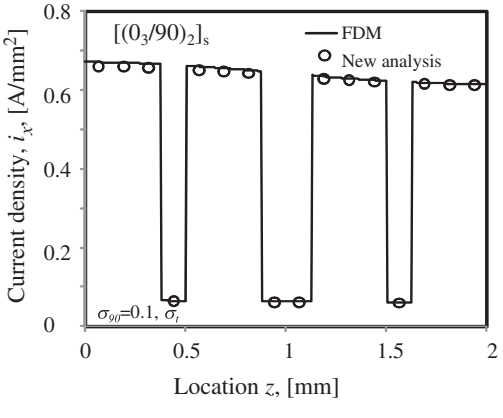

Figure 11. Comparison of the electric current density i_x of Type B at x = 0 mm.

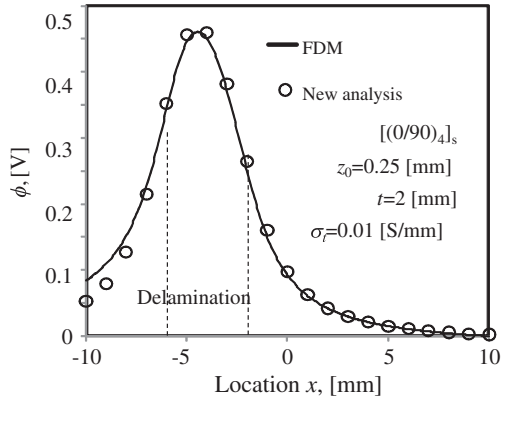

Figure 12. Comparison of the electric potential difference change caused by a delamination crack (Type A, delamination crack location: from −6 to −2 mm).

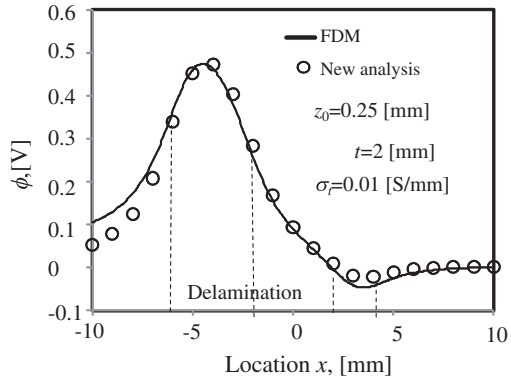

Figure 13. Comparison of the electric potential difference change caused by two delamination cracks (Type A, delamination crack location: from −6 to −2 mm and from 2 to 4 mm).

($x = \pm 10$ mm) are singular points in the analysis, the FDM results include computational error.

From these results, the equivalent electric conductance method for calculating the electric current and potential is proved to be effective for cross-ply laminates.

4. Conclusions

An orthotropic electric potential method was applied to unidirectional CFRP laminates. To improve the method for cross-ply laminates, the equivalent electric conductance that provides the electric potential difference of a cross-ply CFRP laminate is proposed in this study. The effectiveness of the proposed method was investigated using a beam-type specimen. The results were compared with the results obtained by a FDM. The electric current density for two types of cross-ply laminates was calculated and the changes in electric potential difference at the top surface were calculated using orthotropic distributed doublet analysis. The results obtained are as follows:

(1) The new equivalent electric conductance method for calculating the density of the electric current was proposed and the effectiveness of the method proved by comparison with the results of the FDM.
(2) The change in electric potential difference caused by delamination cracking was calculated using orthotropic distributed doublet analysis with the equivalent electric conductance for a cross-ply laminate.

Nomenclature

x	Longitudinal direction
z	Thickness direction
i_x	Electric current density in x-direction
i_z	Electric current density in z-direction
σ_x	Electric conductance in x-direction
σ_z	Electric conductance in z-direction
ϕ	Electric potential

ξ	transformed coordinate in longitudinal direction
η	transformed coordinate in thickness direction
I	Total electric current input
a	Distance of a source or a sink from the center of the specimen
t	Thickness of a ply
N	Number of mirror images
d	Depth of delamination crack from the surface
s	Coordinate of x-direction for integration
x_1	left edge coordinate of delamination crack
x_2	right edge coordinate of delamination crack
V	potential difference
α	Normalized coordinate in the thickness direction
$F(\alpha)$	Contribution function (normalized distribution of electric potential)
C_x	Equivalent electric conductance in the x-direction
n_s	Number of segments for calculation of distributed doublet
x_{cj}	location of the center of the segment number j
$i_z(x_{cj}, d)$	Electric current density of z-direction at x_{cj} of depth of d
μ_j	Strength of doublet at the segment number j
ε	Small distance from the delamination crack in the thickness direction
B_{ij}	Electric current density of unit doublet strength

References

[1] Schulte K, Baron Ch. Load and failure analyses of CFRP laminates by means of electrical resistivity measurements. Compos. Sci. Technol. 1989;36:63–76.
[2] Muto N, Yanagida H, Nakatsuji T, Sugita M, Ohtsuka Y. Preventing fatal fractures in carbon–fibre–glass–fibre–reinforced plastic composites by monitoring change in electrical resistance. J. Am. Ceram. Soc. 1993;76:875–879.
[3] Wang X, Chung DDL. Short carbon fiber reinforced epoxy as a piezoresistive strain sensor. Smart Mater. Struct. 1995;4:363–367.
[4] Todoroki A, Matsuura K, Kobayashi H. Application of electric potential method to smart composite structures for detecting delamination. JSME Int. J. Ser. A 1995;38:524–530.
[5] Irving PE, Thiagarajan C. Fatigue damage characterization in carbon fibre composite materials using an electrical potential technique. Smart Mater. Struct. 1998;7:456–466.
[6] Seo DC, Lee JJ. Damage detection of CFRP laminates using electrical resistance measurement and a neural network. Compos. Struct. 1999;47:525–530.
[7] Abry JC, Choi YK, Chateauminois A, Dalloz B, Giraud G, Salvia M. In-situ monitoring of damage in CFRP laminates by using AC and DC measurements. Compos. Sci. Technol. 2001;61:855–864.
[8] Schueler R, Joshi SP, Schulte K. Damage detection in CFRP by electrical conductivity mapping. Compos. Sci. Technol. 2001;61:921–930.
[9] Park JB, Okabe T, Takeda N, Curtin WA. Electro-mechanical modeling of unidirectional CFRP composites under tensile loading condition. Compos. Part A. 2002;33:267–275.
[10] Todoroki A, Tanaka Y, Shimamura Y. Delamination monitoring of graphite/epoxy laminated composite plate of electric resistance change method. Compos. Sci. Technol. 2002;62: 1151–1160.
[11] Todoroki A, Tanaka Y, Shimamura Y. Delamination monitoring of graphite/epoxy laminated composite plate of electric resistance change method. Compos. Sci. Technol. 2002;62: 1151–1160.
[12] Todoroki A, Tanaka M, Shimamura Y. Measurement of orthotropic electric conductance of CFRP laminates and analysis of the effect on delamination monitoring with electric resistance change method. Compos. Sci. Technol. 2002;62:619–628.
[13] Ogi K, Takao Y. Characterization of piezoresistance behavior in a CFRP unidirectional laminate. Compos. Sci. Technol. 2005;65:231–239.

[14] Angelidis N, Irving PE. Detection of impact damage in CFRP laminates by means of electrical potential techniques. Compos. Sci. Technol. 2007;67:594–604.
[15] Sevkat E, Li J, Liaw B, Delale F. A statistical model of electrical resistance of carbon fiber reinforced composites under tensile loading. Compos. Sci. Technol. 2008;68:2214–2219.
[16] Todoroki A. Electric current analysis of CFRP using perfect fluid potential flow. Trans. Jpn. Soc. Aeronaut. Space Sci. 2012;55:183–190.
[17] Todoroki A. Electric current analysis for thick laminated CFRP composites. Trans. Jpn. Soc. Aeronaut. Space Sci. 2012;55:237–243.
[18] Todoroki A, Arai M. Simple electric-voltage-change-analysis method for delamination of thin CFRP laminates using anisotropic electric potential function. Adv. Compos. Mater. 2014;23:261–273.
[19] Todoroki A. Monitoring of electric conductance and delamination of CFRP using multiple electric potential measurements. Adv. Compos. Mater. 2014;23:179–193.